Molecular Neurobiology (2019) 56:7368–7379
https://doi.org/10.1007/s12035-019-1613-3

S-Ketamine Reverses Hippocampal Dendritic Spine Deficits in Flinders Sensitive Line Rats Within 1 h of Administration

Giulia Treccani[1,2,3] · Maryam Ardalan[1] · Fenghua Chen[1] · Laura Musazzi[4] · Maurizio Popoli[4] · Gregers Wegener[1,5] · Jens Randel Nyengaard[6,7] · Heidi Kaastrup Müller[1]

Received: 19 February 2019 / Accepted: 15 April 2019 / Published online: 29 April 2019

Abstract

When administered as a single subanesthetic dose, the N-methyl-D-aspartate (NMDA) receptor antagonist, ketamine, produces rapid (within hours) and relatively sustained antidepressant actions even in treatment-resistant patients. Preclinical studies have shown that ketamine increases dendritic spine density and synaptic proteins in brain areas critical for the actions of antidepressants, yet the temporal relationship between structural changes and the onset of antidepressant action remains poorly understood. In this study, we examined the effects of a single dose of *S*-ketamine (15 mg/kg) on dendritic length, dendritic arborization, spine density, and spine morphology in the Flinders Sensitive and Flinders Resistant Line (FSL/FRL) rat model of depression. We found that already 1 h after injection with ketamine, apical dendritic spine deficits in CA1 pyramidal neurons of FSL rats were completely restored. Notably, the observed increase in spine density was attributable to regulation of both mushroom and long-thin spines. In contrast, ketamine had no effect on dendritic spine density in FRL rats. On the molecular level, ketamine normalized elevated levels of phospho-cofilin and the NMDA receptor subunits GluN2A and GluN2B and reversed homer3 deficiency in hippocampal synaptosomes of FSL rats. Taken together, our data suggest that rapid formation of new spines may provide an important structural substrate during the initial phase of ketamine's antidepressant action.

Keywords Ketamine · Antidepressants · Dendritic Spines · Synaptosomes · Homer3 · Cofilin

Introduction

Over the past two decades, clinical studies have repeatedly demonstrated that ketamine, a non-competitive antagonist of the N-methyl-D-aspartate (NMDA) receptor, produces rapid, robust, and relatively sustained antidepressant effects in major depressed and treatment-resistant patients, after a single subanesthetic intravenous dose [1–4]. Clinical depression is a serious disorder that affects approximately 16% of the population at some point in life [5, 6], and consequently, the use of ketamine has presented an entirely new approach for reducing depressive symptoms within hours after treatment. In comparison, commonly used

Giulia Treccani and Maryam Ardalan contributed equally to this work.

Electronic supplementary material The online version of this article (https://doi.org/10.1007/s12035-019-1613-3) contains supplementary material, which is available to authorized users.

✉ Heidi Kaastrup Müller
heidi.muller@clin.au.dk

[1] Translational Neuropsychiatry Unit, Department of Clinical Medicine, Aarhus University, Skovagervej 72, 8240 Risskov, Denmark

[2] Department of Psychiatry and Psychotherapy, Johannes Gutenberg University Medical Center Mainz, Untere Zahlbacher Straße 8, Mainz, Germany

[3] Deutsches Resilienz Zentrum (DRZ) gGmbH, Mainz, Germany

[4] Laboratory of Neuropsychopharmacology and Functional Neurogenomics - Dipartimento di Scienze Farmacologiche e Biomolecolari and Center of Excellence on Neurodegenerative Diseases, University of Milano, Milan, Italy

[5] AUGUST Centre, Department of Clinical Medicine, Aarhus University, Risskov, Denmark

[6] Core Center for Molecular Morphology, Section for Stereology and Microscopy, Department of Clinical Medicine, Aarhus University, Aarhus, Denmark

[7] Centre for Stochastic Geometry and Advanced Bioimaging, Aarhus University, Aarhus, Denmark

antidepressant agents are associated with significant limitations including moderate efficacy compared with placebo, low response rates, and delayed onset of action [7]. However, concerns about repeated or chronic intravenous administration and potential psychotomimetic effects of ketamine severely limit its clinical utility. To address this issue, intranasal administration of ketamine is currently under intense investigation as an alternative delivery route, although this does not eliminate dissociative experiences or abuse potential.

Rapid and long-lasting antidepressant properties of ketamine have also been extensively documented in animal models mimicking various symptoms of depression (reviewed in 8, 9), thus providing a platform to obtain mechanistic insight into the cellular and molecular substrates underlying the behavioral actions of ketamine. Accumulating evidence suggests that ketamine can reverse synaptic deficits associated with the pathophysiology of depression by acting at the synaptic level to increase the expression of synaptic proteins and promote structural plasticity in key cortical and limbic brain regions (reviewed in 8,10,11). Although molecular substrates underlying these effects still remain unclear, suggested mechanisms involve activation of α-amino-3-hydroxy-5-methyl-4-isoxazolepropionic acid (AMPA) receptors [12–16], increased expression and release of brain-derived neurotrophic factor (BDNF) [12, 17–20], and activation of the mammalian target of rapamycin (mTOR) [14, 21, 22], which are components known to be implicated in synapse formation and synaptic plasticity.

A key aspect in developing efficient rapid-acting therapies with a safer pharmacological profile than ketamine is to characterize the immediate mechanisms driving ketamine's fast onset of action. The acute antidepressant-like effect of ketamine can be detected within 30 min to 1 h in rodents (reviewed in 8, 9), and while several studies have reported accompanying molecular changes within this time frame, structural synaptic plasticity in terms of alterations in dendritic spines has mainly been investigated at later time points and primarily in cortical areas.

Considering the striking dynamic nature of dendritic spines, which can undergo changes in number and shape on a timescale of minutes to hours in response to altered synaptic activity [23, 24], combined with recent in vitro studies showing that ketamine increases spine size in hippocampal cultures [25] and increases synaptic responses in the CA1 region [26, 27] within 1 h of application, we decided to investigate whether ketamine was able to promote fast dendritic spine remodeling. Therefore, we investigated the impact of a single dose of *S*-ketamine (15 mg/kg) on dendritic arborization, dendritic spine density and morphology in the CA1 area of hippocampus in a genetic rat model displaying depressive-like behavior, the Flinders Sensitive Line (FSL) rat and its control strain, the Flinders Resistant Line (FRL) rat, 1 h post injection. FSL rats were originally bred to have high sensitivity to the anticholinesterase diisopropyl fluorophosphate (DFP), and thus resemble depressed humans with regard to cholinergic supersensitivity [28–31]. Compared with the FSL rats, which exhibit high immobility in the forced swim test (FST), the FRL rats have a lower sensitivity to DFP, and are generally used as the corresponding control line, with low immobility in the FST [32, 33]. The FSL rat model of depression fulfills the major criteria of high face, construct, and predictive validities for research on the pathophysiology of depression [32, 33], including the suppression of neuronal plasticity in the FSL rats [34–37] and response to the main classes of antidepressants [32, 33, 35, 38–41]. In parallel, to shed light on the molecular mechanisms involved in ketamine-induced alterations in dendritic spine dynamics, we analyzed the levels of 18 synaptic plasticity-related proteins in crude synaptosomal preparations from the contralateral hippocampal subregion of the same animals.

Materials and Methods

Animals

Male FSL ($n = 12$) and FRL rats ($n = 12$) (age 11–12 weeks) from our in-house breeding colony were pair-housed in a temperature-controlled (20 ± 2 °C) environment under a 12-h light/dark cycle (lights on at 06:00 a.m.) with ad libitum access to food and water. All animal procedures were carried out under the approval of the Danish National Committee for Ethics in Animal Experimentation (2012-15-2934-00254).

Drug Administration

Animals received a single intraperitoneal injection of ketamine (KET) or saline (control, CNT) between 08:30 and 09:30 a.m. resulting in four experimental groups: FRL CNT, FRL KET, FSL CNT, and FSL KET. Based on previous studies, the clinically used formulation of *S*-ketamine HCl (Pfizer, New York, USA) was used at a dose of 15 mg/kg [40, 41]. The animals were euthanized by decapitation 1 h after injection, and the brains were divided into left and right hemispheres. From each rat, the hippocampus was rapidly dissected from a randomly selected hemisphere and used for molecular studies, while the contralateral hemisphere was processed for rapid Golgi-Cox staining. Continued systematic sampling ensured that groups consisted of an equal distribution of left and right hemispheres.

Morphological Analysis

All analyses were conducted blinded to the experimental conditions. One hemisphere per animal was processed for impregnation of individual neurons using the FD Rapid Golgi Stain TM Kit (FD Neuro Technologies, Inc., Columbia, MD) following the manufacturer's instructions. Hemispheres were sliced coronally (200 μm) on a vibratome (Leica VT1200S

Semiautomatic Vibrating Blade Microtome). Six pyramidal neurons per animal were used for the morphological analysis and were selected from the CA1 stratum radiatum (CA1.SR) subregion of the hippocampus (six pyramidal neurons per animal, a total of 36 neurons per group), and imaged with a digital camera (Olympus DP73) with the newCAST™ system (Visiopharm, Hørsholm, Denmark) using a light microscope (Olympus BX50, Olympus, Denmark) modified for stereology. The identification criteria for the pyramidal neurons were based on the characteristic triangular-shaped soma, having apical dendrites extending toward the pial surface, basal dendrites directed toward stratum oriens, and numerous dendritic spines. Neurons that (1) were separated from neighboring cells without any tangling with dendrites of nearby neurons; (2) presented intact apical and basal dendrites; and (3) had the soma located in the middle of the thickness of the section were sampled by the optical disector, and stacks of images were collected with a *z*-plane step size of 1 μm, using a 60 x oil lens (NA = 1.40) to ensure that dendrites were fully visualized in 3D. In general, there were 100–120 optical layers for each neuron.

Dendrite Reconstructions and Analysis

Captured images were uploaded into Filament Tracer algorithm of the Imaris software (version 8.4.4, Bitplane A.G., Zurich, Switzerland) to perform semi-automatic 3D reconstruction of the dendrites and dendritic spines [42]. All shaft dendritic protrusions (spines) were counted. The morphology of the pyramidal neurons was quantified in terms of the dendritic length and the mean spine density (spines/10 μm). The dendritic spines were additionally classified into three well-described morphological subtypes using the automated Imaris spine classification analysis: stubby spines with a length less than 1 μm, lacking a large spine head and without an apparent neck; mushroom spines with a length less than 3 μm and characterized by a short neck and large spine head; and long-thin spines with mean width of head ≥ mean width of neck and with elongated spine necks. The Sholl analysis [43] was used to provide description of the complexity of the dendritic tree. The analysis was performed based on the regularly spaced concentric circles centered on the neuronal soma. The number of dendritic branch intersections with each progressively larger circle is counted from the soma of each neuron in intervals of 20 μm [44, 45].

Image preparation

Representative z-stacks of 8-bit images were loaded in Fiji (Image J) and converted to an intensity projection along the *z*-axis (min intensity). A square of 50 × 50 μm was cropped representing single dendrites with spines. In all the images, the brightness and contrast of the intensity histogram were set between 20 and 250.

Western Blotting

Crude synaptosomes were prepared from the hippocampus as previously described [46]. Aliquots (20 μg of total protein) were separated on 7.5% or 10% criterion TGX Precast Midi Protein Gels (Bio-Rad), transferred to nitrocellulose membranes using the Trans-Blot Turbo system (Bio-Rad), blocked in Odyssey Blocking Buffer (Licor), and probed with primary antibodies overnight at 4 °C followed by incubation with the appropriate IRDye conjugated secondary antibody (Licor) for 1 h at room temperature (see details in Suppl. Table 1). Infrared signals were detected using the Odyssey CLx infrared imaging system, and bands were quantified using the Image Studio software (LI-COR Biosciences). Band intensities were normalized to β-actin levels within the same lane unless otherwise stated.

Statistics

Morphological data were analyzed using two-way analysis of variance (ANOVA) with strain and ketamine as independent factors. When a significant interaction between independent factors was revealed, Tukey's post hoc test with adjusted *p*-values was applied, considering four comparisons per family (FRL CNT vs. FRL KET; FRL CNT vs. FSL CNT; FRL KET vs. FSL KET; FSL CNT vs. FSL KET). The mean values from the six neurons of each animal in the morphological studies were treated as a single measurement in the data analysis. Sholl analysis was performed using two-way repeated measures ANOVA, with number of intersections as a within-subject factor and the group condition as between-subject factor followed by Bonferroni's post hoc tests with adjusted *p*-values for four comparisons per family. Protein expression levels ($n = 6$ animals per group) were analyzed by two-way ANOVA with Tukey's post hoc test for multiple comparisons (four comparisons per family). All statistical analyses and graphical representations were carried out using Prism 7 (GraphPad Software Inc., USA). Data are expressed as mean ± SEM. An alpha level of 0.05 was used for all statistical tests.

Results

Ketamine Reverses Apical Dendritic Spine Deficits in the Hippocampal CA1 Region of FSL Rats 1 h After Administration

Two-way ANOVA of apical dendritic length revealed a significant interaction between strain and ketamine treatment ($F_{(1,20)} = 5.31$, $p = 0.032$) and no effect of strain ($F_{(1,20)} = 0.47$, $p = 0.498$) or ketamine treatment ($F_{(1,20)} = 0.48$, $p = 0.495$) alone (Fig. 1a). However, Tukey's post hoc test did not yield any significant differences in apical dendritic length after

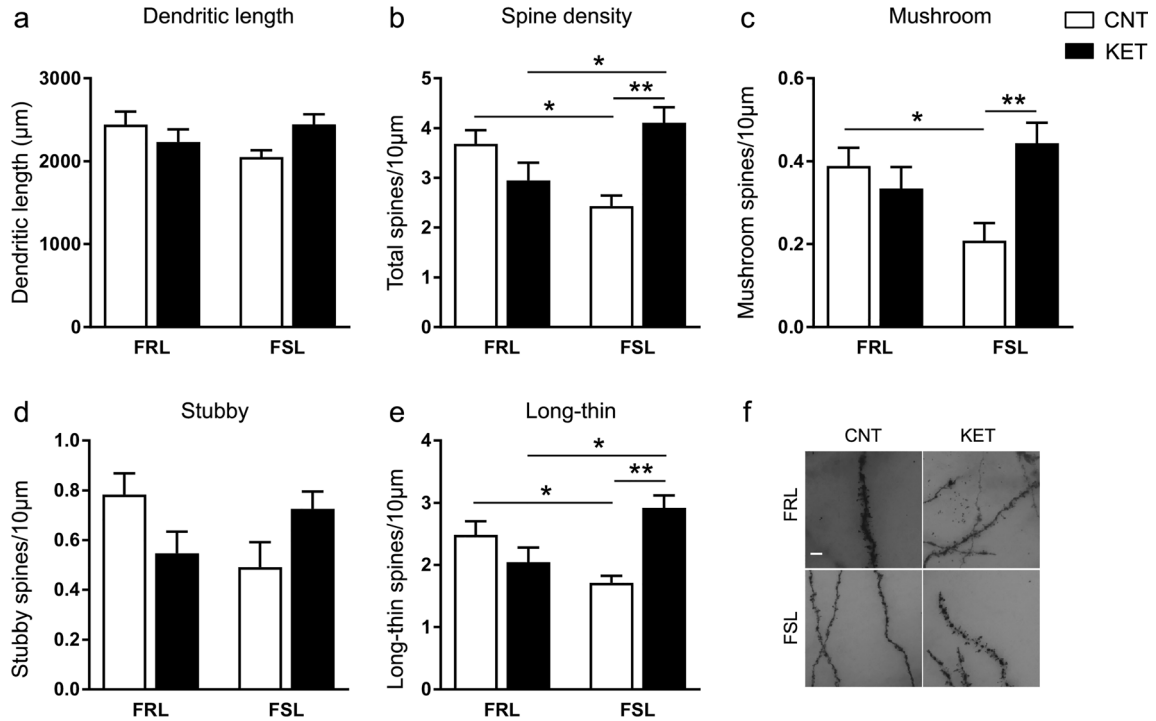

Fig. 1 Ketamine reverses apical dendritic spine deficits in the hippocampal CA1 region of FSL rats 1 h after administration. Apical dendritic length (**a**) and spine density (**b**) in FRL and FSL rats, injected with vehicle or ketamine and sacrificed 1 h later. Analysis of apical dendritic spine morphology, considering mushroom (**c**) stubby (**d**) and long-thin spines (**e**). Representative images of high magnification z-stack projections of apical dendrites (scale: 5 µm) (**f**). Data are presented as mean ± SEM ($n = 6$ animals per group and 6 neurons sampled per animal). *$p < 0.05$, **$p < 0.01$, two-way ANOVA, Tukey's post hoc test

ketamine treatment in either FSL ($p = 0.120$) or FRL ($p = 0.447$) rats. Two-way ANOVA of apical dendritic spine density demonstrated a significant interaction between strain and ketamine treatment ($F_{(1,20)} = 16.82$, $p < 0.001$) with no effect of strain ($F_{(1,20)} = 0.02$, $p = 0.882$) or ketamine treatment ($F_{(1,20)} = 2.58$, $p = 0.124$) alone (Fig. 1b,f). The post hoc analysis revealed reduced spine density in untreated FSL rats compared with untreated FRL rats ($p = 0.022$), which was reversed by ketamine treatment ($p = 0.002$). Ketamine had no effect on spine density in FRL rats ($p = 0.212$), and ketamine-treated FSL rats showed higher spine density than ketamine-treated FRL rats ($p = 0.034$).

To investigate how the differences in apical dendritic spine density between untreated FRL and FSL rats and after ketamine treatment were reflected across different spine subtypes, we classified spines into the three major morphologically distinct types: mushroom, stubby, and long-thin spines. Two-way ANOVA of mushroom spine density revealed a significant interaction between strain and ketamine treatment ($F_{(1,20)} = 9.43$, $p = 0.006$) and no effect of strain ($F_{(1,20)} = 0.57$, $p = 0.46$) or ketamine treatment ($F_{(1,20)} = 3.67$, $p = 0.07$) alone (Fig. 1c). Tukey's post hoc test showed reduced density of mushroom spines in untreated FSL rats compared with untreated FRL rats ($p = 0.040$), which was reversed by ketamine treatment ($p = 0.007$). Ketamine treatment had no effect on mushroom spine density in FRL rats ($p = 0.564$), and mushroom spine density after ketamine treatment did not differ significantly between the two strains ($p = 0.254$). A similar analysis of stubby spine density revealed a significant interaction between strain and ketamine treatment ($F_{(1,20)} = 7.37$, $p = 0.013$) and no effects of strain ($F_{(1,20)} = 0.43$, $p = 0.521$) or ketamine treatment ($F_{(1,20)} = 7.30 \times 10^{-5}$, $p = 0.99$) alone (Fig. 1d). However, post hoc analysis showed that there were no significant differences in the density of stubby spines after ketamine treatment in either FSL rats ($p = 0.17$) or FRL rats ($p = 0.166$). The two-way ANOVA of long-thin spine density revealed a significant interaction between strain and ketamine treatment ($F_{(1,20)} = 17.27$, $p < 0.001$) and no effects of strain ($F_{(1,20)} = 0.07$, $p = 0.794$) or ketamine treatment ($F_{(1,20)} = 3.77$, $p = 0.067$) alone (Fig. 1e). The post hoc test revealed lower density of long-thin spines in untreated FSL rats compared with untreated FRL rats ($p = 0.037$) and that ketamine treatment significantly increased long-thin spine density in FSL rats ($p = 0.001$) but had no effect in FRL rats ($p = 0.28$). In addition, ketamine-treated FSL rats exhibited increased density of long-thin spines compared with ketamine-treated FRL rats ($p = 0.017$).

Ketamine Increases CA1 Basal Dendritic Spine Density Mainly via Induction of Long-Thin Spines

When directing the focus to basal dendrites, a two-way ANOVA showed a significant effect of strain on basal

dendritic length with FSL rats presenting reduced dendritic length compared with FRL rats ($F_{(1,20)} = 6.79$, $p = 0.017$) (Fig. 2a). There was no effect of ketamine treatment and no interaction between strain and ketamine treatment. Two-way ANOVA of basal dendritic spine density showed no significant main effects or significant interaction between strain and ketamine treatment (Fig. 2b,f).

Investigation of the distinct spine subtypes on the basal dendrites showed a significant treatment effect only for the density of long-thin spines (Fig. 2c–e), which increased in response to ketamine treatment ($F_{(1,20)} = 4.72$, $p = 0.042$) (Fig. 2e). There was no effect of strain and no interaction between strain and ketamine treatment on the density of long-thin spines. There was no significant main effect or significant interaction between strain and ketamine treatment for the density of mushroom and stubby spines.

Ketamine Has No Effect on Apical and Basal Dendritic Arborization when Assessed 1 h After Administration

Sholl analysis was performed to investigate dendritic complexity in relation to the distance from the soma. However, two-way ANOVA followed by Bonferroni's post hoc test indicated that ketamine had no significant effect at either apical (Suppl. Fig. 1a) or basal (Suppl. Fig. 1b) dendritic arborization 1 h after administration.

Ketamine Rapidly Restores Reduced Cofilin Phosphorylation and Reverses Altered Expression of homer3 and the NMDA Receptor Subunits GluN2A and GluN2B in the FSL Rats

To shed light on the possible molecular pathways that may contribute to the rapid effects of ketamine on dendritic spine density, we examined the levels of a wide number of synaptic plasticity-related proteins in crude synaptosomes isolated from the contralateral hippocampi of the same animals in which the spine morphology analysis was performed. We focused the analysis on proteins linking synaptic activity to spine morphology, including proteins involved in presynaptic release (syntaxin 1A, SNAP-25, synaptotagmin I, munc-18), signaling protein kinases (phosphorylated and active forms of extracellular regulated kinase [phospho-Erk] and protein kinase B [phospho-Akt]), cell adhesion molecules (neurexin 1 alpha and neuroligin 1), BDNF, and constituents of the postsynaptic machinery (NMDA receptor subunits GluN2A and GluN2B, AMPA receptor subunit GluR1 and its phosphorylation state, cofilin phosphorylation, spinophilin, homer1, homer3, PSD95, and stargazin). Table 1 summarizes the global results of the two-way ANOVA and Tukey's post hoc tests for all targets, while Fig. 3 shows graphs of targets significantly altered by ketamine in FSL rats. For the expression level of the NMDA receptor subunit GluN2A, two-way ANOVA showed a significant interaction between strain and ketamine

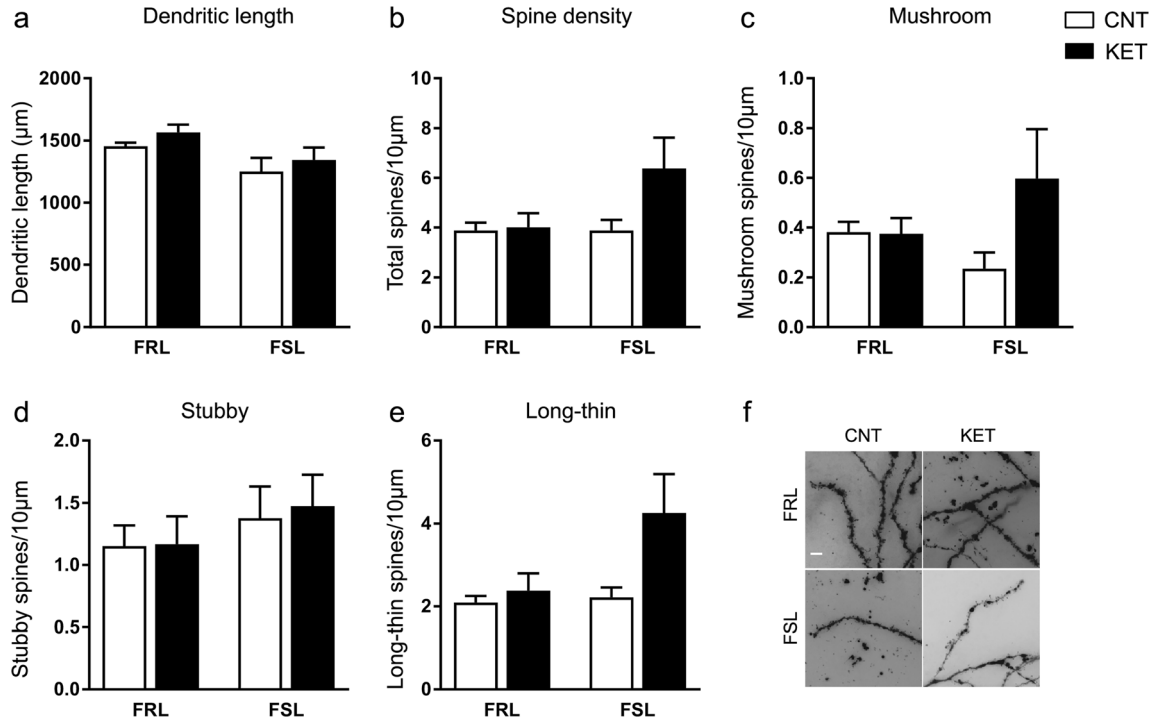

Fig. 2 Ketamine increases CA1 basal dendritic spine density via induction of long-thin spines. Basal dendritic length (**a**) and spine density (**b**) in the same experimental groups as in Fig. 1. Analysis of basal dendritic spine morphology, considering mushroom (**c**) stubby (**d**) and long-thin spines (**e**). Representative images of high magnification z-stack projections of basal dendrites (scale: 5 µm) (**f**). Data are presented as mean ± SEM ($n = 6$ animals per group and 6 neurons sampled per animal), two-way ANOVA

Table 1 Protein levels in crude synaptosomes isolated from the hippocampus of FRL and FSL rats after 1 h of a single injection with vehicle (CNT) or ketamine (KET). Values are mean ± SEM, expressed as percentages of FRL CNT ($n = 6$ animals per group). Two-way ANOVA, Tukey's post hoc test ([a]$p < 0.05$ vs. FRL CNT; [b]$p < 0.05$ vs. FSL CNT; [c]$p < 0.05$ vs. FRL KET; [d]$p < 0.01$ vs. FRL CNT; [e]$p < 0.01$ vs. FSL CNT; [f]$p < 0.001$ vs. FSL CNT). [1]S×D = interaction between strain and treatment

Variable	FRL		FSL		*p* value		
	CNT	KET	CNT	KET	Strain	Treatment	SxD[1]
Syntaxin 1A	100 ± 6.15	103 ± 6.71	108 ± 6.1	108 ± 11.69	0.420	0.851	0.794
SNAP-25	100 ± 8.95	101 ± 2.08	100 ± 4.44	109 ± 2.73	0.465	0.301	0.486
Synaptotagmin I	100 ± 4.53	88.8 ± 1.95	94.7 ± 4.81	105 ± 5.68[c]	0.225	0.944	*0.024*
Munc-18	100 ± 3.04	93.6 ± 4.06	102 ± 2.45	92.7 ± 4.21	0.794	*0.030*	0.608
p-Erk1(Thr202/Tyr204)/Erk	100 ± 2.23	105 ± 5.08	103 ± 2.14	102 ± 3.01	0.790	0.552	0.368
p-Akt(Ser473)/Akt	100 ± 5.53	93.6 ± 5.23	104 ± 4.89	99.2 ± 4.19	0.312	0.247	0.920
Neurexin 1 alpha	100 ± 4.59	90.8 ± 7.58	79.8 ± 4.8	74.26 ± 5.07	*0.004*	0.207	0.751
Neuroligin 1	100 ± 4.3	91.3 ± 2.63	97.4 ± 5.21	100 ± 5.66	0.519	0.514	0.237
BDNF	100 ± 3.2	101 ± 8.12	123 ± 6.76	116 ± 7.23	*0.009*	0.659	0.561
GluN2A	100 ± 2.84	107 ± 4.28	131 ± 4.41[d]	104 ± 7.93[e]	*0.012*	0.076	*0.004*
GluN2B	100 ± 2.1	121 ± 11.25	135 ± 5.84[a]	101 ± 11.66[b]	0.415	0.499	*0.006*
GluR1	100 ± 2.37	91 ± 3.41	98.8 ± 2.13	97 ± 2.65	0.393	0.058	0.200
p-GluR1(Ser831)/GluR1	100 ± 5.18	102 ± 3.77	104 ± 2.33	104 ± 3.16	0.421	0.612	0.794
p-GluR1(Ser845)/GluR1	100 ± 7.86	116 ± 3.89	110 ± 6.28	112 ± 4.32	0.604	0.112	0.237
p-cofilin(Ser3)/cofilin	100 ± 5.30	103 ± 6.18	127 ± 4.58[d]	105 ± 4.79[b]	*0.010*	0.077	*0.030*
Cofilin	100 ± 6.94	96.3 ± 4.34	95.7 ± 3.96	102 ± 3.86	0.897	0.799	0.3263
Spinophilin	100 ± 2.1	107 ± 6.78	103 ± 2.62	93.2 ± 2.94	0.224	0.683	*0.045*
Homer1	100 ± 0.86	99.6 ± 1.9	95.2 ± 1.7	93.8 ± 1.21[c]	*0.002*	0.531	0.741
Homer3	100 ± 4.79	104 ± 2.24	85.3 ± 4.32[a]	112 ± 1.65[f]	0.357	*< 0.001*	*0.004*
PSD95	100 ± 4.04	97.8 ± 2.61	94.2 ± 6.2	91 ± 5.68	0.210	0.584	0.927
Stargazin	100 ± 6.65	96 ± 8.08	85 ± 6.76	90.9 ± 2.08	0.127	0.885	0.444

treatment ($F_{(1,20)} = 10.43$, $p = 0.004$), a significant effect of strain ($F_{(1,20)} = 7.69$, $p = 0.012$), but no effect of treatment alone (Fig. 3a,e and Table 1). The post hoc analysis revealed higher expression levels of GluN2A in untreated FSL rats compared with untreated FRL rats ($p = 0.001$), while ketamine reduced GluN2A levels to FRL control levels ($p = 0.006$). The analysis of the GluN2B subunit showed a significant interaction between strain and ketamine treatment ($F_{(1,20)} = 9.51$, $p = 0.006$) with no effect of strain and ketamine treatment alone (Fig. 3b,e and Table 1). Similar to GluN2A, the post hoc analysis revealed higher levels of GluN2B in untreated FSL rats compared with untreated FRL rats ($p = 0.035$), which was reversed by ketamine treatment ($p = 0.043$). For homer3, there was a significant interaction between strain and ketamine treatment ($F_{(1,20)} = 10.47$, $p = 0.004$), a significant effect of treatment ($F_{(1,20)} = 21.05$, $p < 0.001$), but no effect of strain alone (Fig. 3c,e and Table 1). The post hoc analysis revealed lower levels of homer3 in untreated FSL rats compared with untreated FRL rats ($p = 0.024$), which was rescued by ketamine treatment ($p < 0.001$). The analysis of the phosphorylation state of cofilin, which indirectly reflects its activity, showed a significant interaction between strain and ketamine treatment ($F_{(1,20)} = 5.44$, $p = 0.030$), a significant effect of strain ($F_{(1,20)} = 8.21$, $p = 0.01$), but no effect of treatment alone (Fig. 3d,e and Table 1). The post hoc analysis revealed increased phosphorylation of cofilin in untreated FSL rats compared with untreated FRL rats ($p = 0.005$), which was normalized to FRL levels by ketamine treatment ($p = 0.023$).

DISCUSSION

The present findings demonstrate that a single injection of ketamine rescues morphological deficits of pyramidal neurons in the hippocampal CA1 area of FSL rats as early as 1 h after administration, which coincides with the onset of antidepressant-like effects in the same model [39–41]. Ketamine-induced spinogenesis in the apical dendritic tree was selective for FSL rats and was related to increases in mushroom and long-thin spines. Generally, there were no significant effects of ketamine on dendritic length and branching complexity consistent with the short time interval. The ketamine-induced increase in dendritic spine density in FSL rats was associated with a reduction of synaptic levels of

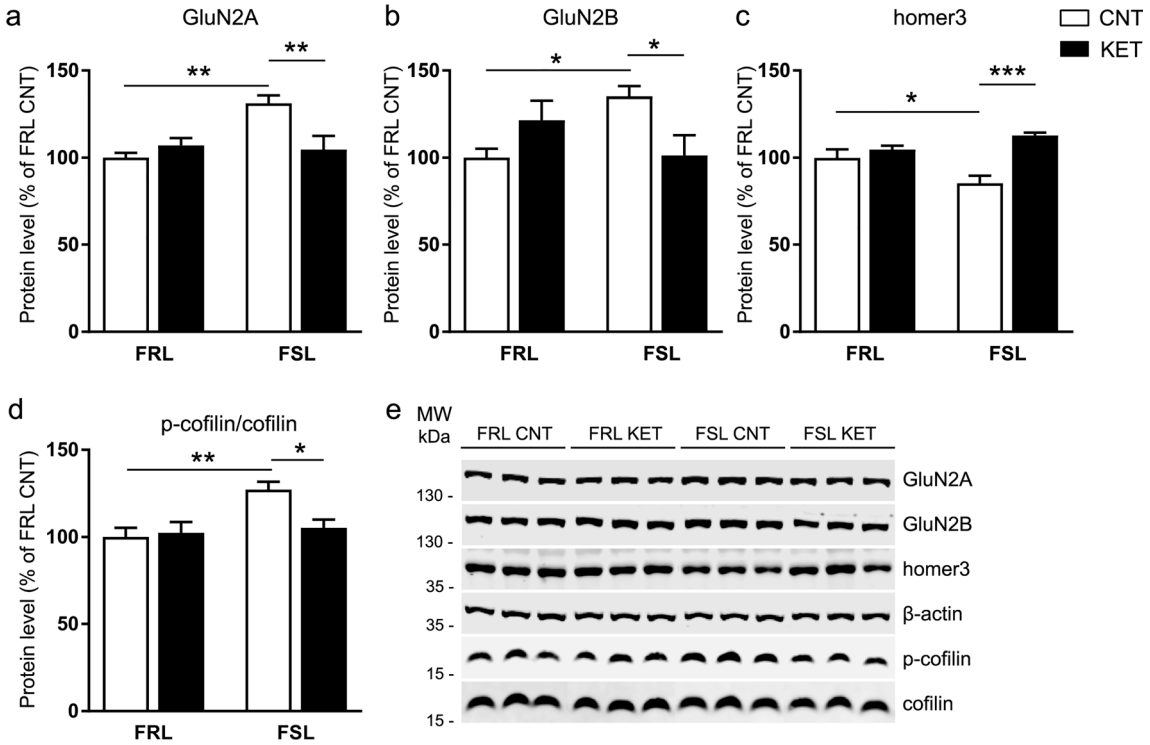

Fig. 3 Ketamine rescues aberrant levels of synaptic proteins in FSL rats after 1 h of administration. Bar graphs representing the β-actin normalized density of GluN2A (**a**), GluN2B (**b**), homer3 (**c**), and phospho-cofilin (p-cofilin) normalized to total cofilin (**d**) in preparations of crude synaptosomal fractions isolated from the hippocampus. **e** Representative Western blots of the individual proteins. Values are means ± SEM ($n = 6$ per group), expressed as percentages of FRL CNT. *$p < 0.05$, **$p < 0.01$, ***$p < 0.001$, two-way ANOVA, Tukey's post hoc test

NMDA receptor subunits GluN2A and GluN2B and cofilin phosphorylation (which were upregulated in untreated FSL rats), together with increased homer3 protein expression levels (where basal levels were found to be lower in FSL rats compared with FRL rats).

A Link Between Fast Spine Remodeling and Ketamine's Antidepressant Effect in FSL Rats

Postmortem studies suggest that depression is closely associated with synaptic atrophy, resulting in disconnection of critical cortical-limbic circuits [47–49]. Similar features are recapitulated in rodents subjected to chronic stress paradigms, where depression-like behavior is generally accompanied by dendritic atrophy and spine loss in neurons of the hippocampus and prefrontal cortex (reviewed in 50, 51). Accordingly, we have previously shown that FSL rats have volumetric reductions and a lower number of spine synapses in the CA1 region of the hippocampus compared with FRL rats [34–37].

In the present study, we provide additional evidence of synaptic alterations in FSL rats by demonstrating a decrease in dendritic spine density in the CA1 area. Here, we also found that ketamine is able to completely rescue spine deficiency in FSL rats in just 1 h.

We have previously shown that a single injection of *S*-ketamine (15 mg/kg), the same treatment used here, reduces immobility of FSL rats in the FST 1 h post injection [39–41]. This is in line with previous reports [18, 52–55], demonstrating that ketamine induces an antidepressant-like response within 1 h after administration in rats.

For the first time, the present results show that spine remodeling occurs at the same time as the onset of ketamine's antidepressant-like effect, suggesting that dendritic spine dynamics may contribute to fast antidepressant action. A previous in vitro study showed that application of 2.0 μm ketamine to cultured hippocampal neurons for 1 h induced an increase in dendritic spine size, but contrary to our findings, there were no changes in spine density at this time point [25]. The authors also reported similar effects after treatment of hippocampal neurons with vortioxetine despite in vivo reports of increased spine density in response to this drug. This discrepancy could be ascribed to the difficulty in extrapolating in vivo drug concentrations to comparable in vitro doses but could also suggest that the integration of signals necessary to promote spine formation in response to ketamine (and possibly other drugs) is dependent on a more complex three-dimensional environment, not present in cultured neurons. In contrast to our study, previous

in vivo studies have mainly investigated structural remodeling in response to acute ketamine over a time scale of several hours to days. When analyzed after 24 h, ketamine (10 mg/kg) was shown to increase cortical spine density in naive animals [21, 56–58] and reverse deficits in spine density induced by chronic unpredictable stress in the prefrontal cortex [59] and hippocampus [60]. Longer lasting or delayed effects were demonstrated after 8 days in the social defeat stress model, in which ketamine (10 mg/kg) reversed the reduction in spine density in cortical and hippocampal regions [61, 62].

In addition, we have previously shown that acute ketamine (15 mg/kg [S-KET]) administration induces a rapid (after 1 day) and long lasting (up to 7 days) increase in the number of excitatory synapses in FSL rats [34, 35]. Moreover, a recent study by Sarkar and Kabbaj demonstrated that even a relatively low dose of ketamine (5 mg/kg) was able to rescue isolation stress evoked deficits in prefrontal cortex spine density at 3 h post-injection [63]. In the same study, the increase of spine density after ketamine treatment was significant only in stressed rats and not in the control pair-housed rats, as also found in the present study, in which ketamine increased spine density only in FSL rats and not in the FRL control rats. This could explain why a recent study investigating the effect of ketamine in naive rats did not reveal any changes in spine density in hippocampus and prefrontal cortex 3 h after treatment [64]. Similarly, ketamine had no immediate effects on spine growth when analyzed by two-photon imaging in naive mice [65].

Therefore, we speculate that ketamine may exert its rapid actions on spine dynamics only in a context of impaired structural plasticity, possibly by tilting the balance between spine formation and elimination, with a net gain in the number of dendritic spines. In this context, it is however interesting to notice that cannabidiol, which induces a rapid and sustained antidepressant-like effect in rodents similar to ketamine, has been shown to increase spine density in the prefrontal cortex of naive mice already after 30 min [66].

Dendritic spines are highly dynamic structures, which can undergo morphological changes and de novo formation/pruning over periods of hours and even minutes in response to synaptic stimuli [23, 24, 67, 68]. Although the temporal relationship between the development of new spines and the formation of functional synapses remains poorly defined, evidence is accumulating supporting that new spines are rapidly incorporated into functional synapses [23, 68–70]. It would be interesting to assess if the rapid increase in the number of spines we found is associated with the generation of new functional synapses.

The classification of spines as having mushroom, stubby, or long-thin morphologies, allowed us to reveal significant increases in mushroom and long-thin spine subtypes in FSL rats after ketamine treatment, thus reflecting changes in both mature and immature spines. This was, however, specific for the apical dendritic tree. Apical and basal dendrites of CA1 pyramidal cells are functionally and spatially separated compartments that receive information from distinct sources and differ significantly in the mechanisms regulating synaptic plasticity [71]. Consequently, our findings could suggest that ketamine primarily targets inputs controlling synaptic plasticity in apical dendrites.

Synaptic Molecular Alterations Associated with Fast Ketamine-Induced Spine Remodeling in FSL Rats

Increased translation and release of the neurotrophic factor BDNF in the hippocampus was demonstrated to play a key role for the rapid antidepressant action of ketamine [14, 17, 18, 72]. However, in the present study, ketamine had no effect on synaptosomal BDNF levels 1 h after administration. This apparent discrepancy between our study and previous reports may be ascribed to tissue processing. We studied crude synaptosomal fractions as opposed to total homogenate, which was used in the studies reporting increased BDNF levels in response to ketamine. BDNF levels measured in synaptosomes mainly represent BDNF localized to the presynaptic compartment. In contrast, total homogenate may capture increased translation and secretion of BDNF from other compartments of the synapse including postsynaptic dendrites, astrocytes, and microglia. In this context, it is interesting to note that ketamine has been speculated to selectively enhance a postsynaptic pool of BDNF [73], in which case it will not be revealed in synaptosomal preparations. In addition, the use of *S*-ketamine versus racemic ketamine and the doses applied may influence BDNF levels differently.

Regarding NMDA receptor subunits, we previously reported decreased GluN2A and increased GluN2B levels in postsynaptic membrane-enriched hippocampal fractions of FSL rat [74]. In the present study, we found increased levels of both subunits in crude synaptosomes (a fraction enriched in pre-synaptic terminals), consistent with altered glutamatergic transmission in the FSL rat strain [75–77]. We found that ketamine restored the elevated levels of GluN2A and GluN2B in synaptosomes of FSL rats 1 h after administration, suggesting normalization of aberrant NMDA receptor function in FSL rats. Given the short time frame (1 h after treatment), we speculate that this decrease in synaptosomal levels of NMDA receptor subunits reflects rapid cellular redistribution of NMDA receptors to extrasynaptic sites (or locations not captured in the synaptosomal preparation) rather than changes in protein translation.

Homer3 is a scaffold protein involved in the binding of signaling molecules at the postsynaptic densities. Our biochemical studies revealed that ketamine restored reduced levels of homer3 in FSL rats. Interestingly, synaptic clustering of homer proteins has previously been shown to be enhanced by blockade of NMDA receptors [78]. This effect of ketamine could be in line with increased synaptic strength. Finally, we showed that ketamine normalized elevated Ser-3 phosphorylation levels of the actin-binding protein cofilin in FSL rats. Phospho-regulation of cofilin is a key effector linking extracellular stimuli to actin dynamics in dendritic spines, which directly regulate spine morphology and drives formation and elimination of spines [79]. Because the activity of cofilin is negatively regulated by phosphorylation, ketamine appears to restore cofilin's actin-severing activity, which could be an important mediator in the induction of new spines observed after ketamine treatment.

Collectively, our findings indicate that hippocampal structural remodeling in terms of rapid de novo spine growth may provide an important substrate during the initial phase of ketamine's antidepressant action and thus supports the synaptogenic hypothesis of treatment response [80]. In addition, we identify a possible link between the rapid actions of ketamine and downregulation of NMDA receptor subunits, increased homer3 levels and normalization of cofilin activity.

Acknowledgments Centre for Stochastic Geometry and Advanced Bioimaging is supported by Villum Foundation. We gratefully acknowledge the support by the Core Facility Microscopy of the Institute of Molecular Biology (IMB) in Mainz, Germany and Ferruccio Bosetti for IT consulting. We thank Maiken Krogsbæk Mikkelsen for her assistance with microscopy.

Author Contributions G.T., M.A., and H.K.M performed the experiments, analyzed and interpreted the results. G.T. and H.K.M. wrote the paper. All co-authors provided conceptual advice, commented on the manuscript, and approved the final version before submission.

Funding Information Funding was provided for G.T. by a NARSAD Young Investigator Grant from the Brain & Behavior Research Foundation and a postdoctoral research grant from the Danish Council for Independent Research (DFF–5053-00103). L.M. was supported by CARIPLO Foundation (Biomedical Science for Young Scientists, Prog. 2014-1133). The work was supported by grants from Dagmar Marshall's Foundation, Direktør Jacob Madsen and Hustru Olga Madsen's Foundation, Aase og Ejnar Danielsen's Foundation, Kong Christian den Tiendes Foundation, and Direktør Kurt Bønnelycke and Hustru Fru Grethe Bønnelycke's Foundation.

References

1. Berman RM, Cappiello A, Anand A, Oren DA, Heninger GR, Charney DS, Krystal JH (2000) Antidepressant effects of ketamine in depressed patients. Biol Psychiatry 47(4):351–354
2. DiazGranados N, Ibrahim LA, Brutsche NE, Ameli R, Henter ID, Luckenbaugh DA, Machado-Vieira R, Zarate CA Jr (2010) Rapid resolution of suicidal ideation after a single infusion of an N-methyl-D-aspartate antagonist in patients with treatment-resistant major depressive disorder. J Clin Psychiatry 71(12):1605–1611. https://doi.org/10.4088/JCP.09m05327blu
3. Price RB, Iosifescu DV, Murrough JW, Chang LC, Al Jurdi RK, Iqbal SZ, Soleimani L, Charney DS et al (2014) Effects of ketamine on explicit and implicit suicidal cognition: a randomized controlled trial in treatment-resistant depression. Depress Anxiety 31(4):335–343. https://doi.org/10.1002/da.22253
4. Zarate CA Jr, Singh JB, Carlson PJ, Brutsche NE, Ameli R, Luckenbaugh DA, Charney DS, Manji HK (2006) A randomized trial of an N-methyl-D-aspartate antagonist in treatment-resistant major depression. Arch Gen Psychiatry 63(8):856–864. https://doi.org/10.1001/archpsyc.63.8.856
5. Kessler RC, Berglund P, Demler O, Jin R, Koretz D, Merikangas KR, Rush AJ, Walters EE et al (2003) The epidemiology of major depressive disorder: results from the National Comorbidity Survey Replication (NCS-R). JAMA 289(23):3095–3105. https://doi.org/10.1001/jama.289.23.3095
6. Lim GY, Tam WW, Lu Y, Ho CS, Zhang MW, Ho RC (2018) Prevalence of depression in the community from 30 countries between 1994 and 2014. Sci Rep 8(1):2861. https://doi.org/10.1038/s41598-018-21243-x
7. Trivedi MH, Rush AJ, Wisniewski SR, Nierenberg AA, Warden D, Ritz L, Norquist G, Howland RH et al (2006) Evaluation of outcomes with citalopram for depression using measurement-based care in STAR*D: implications for clinical practice. Am J Psychiatry 163(1):28–40. https://doi.org/10.1176/appi.ajp.163.1.28
8. Browne CA, Lucki I (2013) Antidepressant effects of ketamine: mechanisms underlying fast-acting novel antidepressants. Front Pharmacol 4:161. https://doi.org/10.3389/fphar.2013.00161
9. Saland SK, Duclot F, Kabbaj M (2017) Integrative analysis of sex differences in the rapid antidepressant effects of ketamine in preclinical models for individualized clinical outcomes. Curr Opin Behav Sci 14:19–26. https://doi.org/10.1016/j.cobeha.2016.11.002
10. Zanos P, Gould TD (2018) Mechanisms of ketamine action as an antidepressant. Mol Psychiatry 23(4):801–811. https://doi.org/10.1038/mp.2017.255
11. Kadriu B, Musazzi L, Henter ID, Graves M, Popoli M, Zarate CA Jr (2018) Glutamatergic neurotransmission: pathway to developing novel rapid-acting antidepressant treatments. Int J Neuropsychopharmacol 22:119–135. https://doi.org/10.1093/ijnp/pyy094
12. Zanos P, Moaddel R, Morris PJ, Georgiou P, Fischell J, Elmer GI, Alkondon M, Yuan P et al (2016) NMDAR inhibition-independent antidepressant actions of ketamine metabolites. Nature 533(7604):481–486. https://doi.org/10.1038/nature17998
13. Maeng S, Zarate CA Jr, Du J, Schloesser RJ, McCammon J, Chen G, Manji HK (2008) Cellular mechanisms underlying the antidepressant effects of ketamine: role of alpha-amino-3-hydroxy-5-methylisoxazole-4-propionic acid receptors. Biol Psychiatry 63(4):349–352. https://doi.org/10.1016/j.biopsych.2007.05.028
14. Zhou W, Wang N, Yang C, Li XM, Zhou ZQ, Yang JJ (2014) Ketamine-induced antidepressant effects are associated with AMPA receptors-mediated upregulation of mTOR and BDNF in rat hippocampus and prefrontal cortex. Eur Psychiatry 29(7):419–423. https://doi.org/10.1016/j.eurpsy.2013.10.005
15. Koike H, Iijima M, Chaki S (2011) Involvement of AMPA receptor in both the rapid and sustained antidepressant-like effects of ketamine in animal models of depression. Behav Brain Res 224(1):107–111. https://doi.org/10.1016/j.bbr.2011.05.035
16. Walker AK, Budac DP, Bisulco S, Lee AW, Smith RA, Beenders B, Kelley KW, Dantzer R (2013) NMDA receptor blockade by ketamine abrogates lipopolysaccharide-induced depressive-like behavior in C57BL/6J mice. Neuropsychopharmacology 38(9):1609–1616. https://doi.org/10.1038/npp.2013.71

17. Autry AE, Adachi M, Nosyreva E, Na ES, Los MF, Cheng PF, Kavalali ET, Monteggia LM (2011) NMDA receptor blockade at rest triggers rapid behavioural antidepressant responses. Nature 475(7354):91–95. https://doi.org/10.1038/nature10130
18. Garcia LS, Comim CM, Valvassori SS, Reus GZ, Barbosa LM, Andreazza AC, Stertz L, Fries GR et al (2008) Acute administration of ketamine induces antidepressant-like effects in the forced swimming test and increases BDNF levels in the rat hippocampus. Prog Neuro-Psychopharmacol Biol Psychiatry 32(1):140–144. https://doi.org/10.1016/j.pnpbp.2007.07.027
19. Liu RJ, Lee FS, Li XY, Bambico F, Duman RS, Aghajanian GK (2012) Brain-derived neurotrophic factor Val66Met allele impairs basal and ketamine-stimulated synaptogenesis in prefrontal cortex. Biol Psychiatry 71(11):996–1005. https://doi.org/10.1016/j.biopsych.2011.09.030
20. Lepack AE, Fuchikami M, Dwyer JM, Banasr M, Duman RS (2014) BDNF release is required for the behavioral actions of ketamine. Int J Neuropsychopharmacol 18(1):pyu033. https://doi.org/10.1093/ijnp/pyu033
21. Li N, Lee B, Liu RJ, Banasr M, Dwyer JM, Iwata M, Li XY, Aghajanian G et al (2010) mTOR-dependent synapse formation underlies the rapid antidepressant effects of NMDA antagonists. Science 329(5994):959–964. https://doi.org/10.1126/science.1190287
22. Paul RK, Singh NS, Khadeer M, Moaddel R, Sanghvi M, Green CE, O'Loughlin K, Torjman MC et al (2014) (R,S)-Ketamine metabolites (R,S)-norketamine and (2S,6S)-hydroxynorketamine increase the mammalian target of rapamycin function. Anesthesiology 121(1):149–159. https://doi.org/10.1097/ALN.0000000000000285
23. Zito K, Scheuss V, Knott G, Hill T, Svoboda K (2009) Rapid functional maturation of nascent dendritic spines. Neuron 61(2):247–258. https://doi.org/10.1016/j.neuron.2008.10.054
24. Fischer M, Kaech S, Knutti D, Matus A (1998) Rapid actin-based plasticity in dendritic spines. Neuron 20(5):847–854
25. Waller JA, Chen F, Sanchez C (2016) Vortioxetine promotes maturation of dendritic spines in vitro: a comparative study in hippocampal cultures. Neuropharmacology 103:143–154. https://doi.org/10.1016/j.neuropharm.2015.12.012
26. Widman AJ, McMahon LL (2018) Disinhibition of CA1 pyramidal cells by low-dose ketamine and other antagonists with rapid antidepressant efficacy. Proc Natl Acad Sci U S A 115(13):E3007–E3016. https://doi.org/10.1073/pnas.1718883115
27. Nosyreva E, Szabla K, Autry AE, Ryazanov AG, Monteggia LM, Kavalali ET (2013) Acute suppression of spontaneous neurotransmission drives synaptic potentiation. J Neurosci 33(16):6990–7002. https://doi.org/10.1523/JNEUROSCI.4998-12.2013
28. Janowsky DS, Overstreet DH, Nurnberger JI Jr (1994) Is cholinergic sensitivity a genetic marker for the affective disorders? Am J Med Genet 54(4):335–344. https://doi.org/10.1002/ajmg.1320540412
29. Overstreet DH (1986) Selective breeding for increased cholinergic function: development of a new animal model of depression. Biol Psychiatry 21(1):49–58
30. Overstreet DH, Russell RW (1982) Selective breeding for diisopropyl fluorophosphate-sensitivity: behavioural effects of cholinergic agonists and antagonists. Psychopharmacology 78(2):150–155
31. Overstreet DH, Russell RW, Helps SC, Messenger M (1979) Selective breeding for sensitivity to the anticholinesterase DFP. Psychopharmacology 65(1):15–20
32. Wegener G, Mathe AA, Neumann ID (2012) Selectively bred rodents as models of depression and anxiety. Curr Top Behav Neurosci 12:139–187. https://doi.org/10.1007/7854_2011_192
33. Overstreet DH, Wegener G (2013) The flinders sensitive line rat model of depression–25 years and still producing. Pharmacol Rev 65(1):143–155. https://doi.org/10.1124/pr.111.005397
34. Ardalan M, Wegener G, Polsinelli B, Madsen TM, Nyengaard JR (2016) Neurovascular plasticity of the hippocampus one week after a single dose of ketamine in genetic rat model of depression. Hippocampus 26(11):1414–1423. https://doi.org/10.1002/hipo.22617
35. Ardalan M, Wegener G, Rafati AH, Nyengaard JR (2017) S-Ketamine rapidly reverses synaptic and vascular deficits of hippocampus in genetic animal model of depression. Int J Neuropsychopharmacol 20(3):247–256. https://doi.org/10.1093/ijnp/pyw098
36. Chen F, Ardalan M, Elfving B, Wegener G, Madsen TM, Nyengaard JR (2018) Mitochondria are critical for BDNF-mediated synaptic and vascular plasticity of hippocampus following repeated electroconvulsive seizures. Int J Neuropsychopharmacol 21(3):291–304. https://doi.org/10.1093/ijnp/pyx115
37. Chen F, Madsen TM, Wegener G, Nyengaard JR (2010) Imipramine treatment increases the number of hippocampal synapses and neurons in a genetic animal model of depression. Hippocampus 20(12):1376–1384. https://doi.org/10.1002/hipo.20718
38. Ardalan M, Rafati AH, Nyengaard JR, Wegener G (2017) Rapid antidepressant effect of ketamine correlates with astroglial plasticity in the hippocampus. Br J Pharmacol 174(6):483–492. https://doi.org/10.1111/bph.13714
39. Liebenberg N, Joca S, Wegener G (2015) Nitric oxide involvement in the antidepressant-like effect of ketamine in the Flinders sensitive line rat model of depression. Acta Neuropsychiatr 27(2):90–96. https://doi.org/10.1017/neu.2014.39
40. du Jardin KG, Liebenberg N, Cajina M, Müller HK, Elfving B, Sanchez C, Wegener G (2017) S-Ketamine mediates its acute and sustained antidepressant-like activity through a 5-HT1B receptor dependent mechanism in a genetic rat model of depression. Front Pharmacol 8:978. https://doi.org/10.3389/fphar.2017.00978
41. du Jardin KG, Liebenberg N, Müller HK, Elfving B, Sanchez C, Wegener G (2016) Differential interaction with the serotonin system by S-ketamine, vortioxetine, and fluoxetine in a genetic rat model of depression. Psychopharmacology 233(14):2813–2825. https://doi.org/10.1007/s00213-016-4327-5
42. Al-Absi AR, Christensen HS, Sanchez C, Nyengaard JR (2018) Evaluation of semi-automatic 3D reconstruction for studying geometry of dendritic spines. J Chem Neuroanat 94:119–124. https://doi.org/10.1016/j.jchemneu.2018.10.008
43. Sholl DA (1953) Dendritic organization in the neurons of the visual and motor cortices of the cat. J Anat 87(4):387–406
44. Chen F, du Jardin KG, Waller JA, Sanchez C, Nyengaard JR, Wegener G (2016) Vortioxetine promotes early changes in dendritic morphology compared to fluoxetine in rat hippocampus. Eur Neuropsychopharmacol 26(2):234–245. https://doi.org/10.1016/j.euroneuro.2015.12.018
45. Nava N, Treccani G, Alabsi A, Müller HK, Elfving B, Popoli M, Wegener G, Nyengaard JR (2017) Temporal dynamics of acute stress-induced dendritic remodeling in medial prefrontal cortex and the protective effect of desipramine. Cereb Cortex 27(1):694–705. https://doi.org/10.1093/cercor/bhv254
46. Müller HK, Wegener G, Liebenberg N, Zarate CA Jr, Popoli M, Elfving B (2013) Ketamine regulates the presynaptic release machinery in the hippocampus. J Psychiatr Res 47(7):892–899. https://doi.org/10.1016/j.jpsychires.2013.03.008
47. Kang HJ, Voleti B, Hajszan T, Rajkowska G, Stockmeier CA, Licznerski P, Lepack A, Majik MS et al (2012) Decreased expression of synapse-related genes and loss of synapses in major

depressive disorder. Nat Med 18(9):1413–1417. https://doi.org/10.1038/nm.2886
48. MacQueen G, Frodl T (2011) The hippocampus in major depression: evidence for the convergence of the bench and bedside in psychiatric research? Mol Psychiatry 16(3):252–264. https://doi.org/10.1038/mp.2010.80
49. Price JL, Drevets WC (2010) Neurocircuitry of mood disorders. Neuropsychopharmacology 35(1):192–216. https://doi.org/10.1038/npp.2009.104
50. Qiao H, Li MX, Xu C, Chen HB, An SC, Ma XM (2016) Dendritic spines in depression: what we learned from animal models. Neural Plast 2016:8056370. https://doi.org/10.1155/2016/8056370
51. Musazzi L, Treccani G, Popoli M (2015) Functional and structural remodeling of glutamate synapses in prefrontal and frontal cortex induced by behavioral stress. Front Psychiatry 6:60. https://doi.org/10.3389/fpsyt.2015.00060
52. Walker AJ, Foley BM, Sutor SL, McGillivray JA, Frye MA, Tye SJ (2015) Peripheral proinflammatory markers associated with ketamine response in a preclinical model of antidepressant-resistance. Behav Brain Res 293:198–202. https://doi.org/10.1016/j.bbr.2015.07.026
53. Zhou W, Dong L, Wang N, Shi JY, Yang JJ, Zuo ZY, Zhou ZQ (2014) Akt mediates GSK-3beta phosphorylation in the rat prefrontal cortex during the process of ketamine exerting rapid antidepressant actions. Neuroimmunomodulation 21(4):183–188. https://doi.org/10.1159/000356517
54. Yang Y, Cui Y, Sang K, Dong Y, Ni Z, Ma S, Hu H (2018) Ketamine blocks bursting in the lateral habenula to rapidly relieve depression. Nature 554(7692):317–322. https://doi.org/10.1038/nature25509
55. Burgdorf J, Zhang XL, Nicholson KL, Balster RL, Leander JD, Stanton PK, Gross AL, Kroes RA et al (2013) GLYX-13, a NMDA receptor glycine-site functional partial agonist, induces antidepressant-like effects without ketamine-like side effects. Neuropsychopharmacology 38(5):729–742. https://doi.org/10.1038/npp.2012.246
56. Liu RJ, Fuchikami M, Dwyer JM, Lepack AE, Duman RS, Aghajanian GK (2013) GSK-3 inhibition potentiates the synaptogenic and antidepressant-like effects of subthreshold doses of ketamine. Neuropsychopharmacology 38(11):2268–2277. https://doi.org/10.1038/npp.2013.128
57. Ruddy RM, Chen Y, Milenkovic M, Ramsey AJ (2015) Differential effects of NMDA receptor antagonism on spine density. Synapse 69(1):52–56. https://doi.org/10.1002/syn.21784
58. Phoumthipphavong V, Barthas F, Hassett S, Kwan AC (2016) Longitudinal effects of ketamine on dendritic architecture in vivo in the mouse medial frontal cortex. eNeuro 3(2). https://doi.org/10.1523/ENEURO.0133-15.2016
59. Li N, Liu RJ, Dwyer JM, Banasr M, Lee B, Son H, Li XY, Aghajanian G et al (2011) Glutamate N-methyl-D-aspartate receptor antagonists rapidly reverse behavioral and synaptic deficits caused by chronic stress exposure. Biol Psychiatry 69(8):754–761. https://doi.org/10.1016/j.biopsych.2010.12.015
60. Zhang WJ, Wang HH, Lv YD, Liu CC, Sun WY, Tian LJ (2018) Downregulation of Egr-1 expression level via GluN2B underlies the antidepressant effects of ketamine in a chronic unpredictable stress animal model of depression. Neuroscience 372:38–45. https://doi.org/10.1016/j.neuroscience.2017.12.045
61. Yang C, Shirayama Y, Zhang JC, Ren Q, Yao W, Ma M, Dong C, Hashimoto K (2015) R-ketamine: a rapid-onset and sustained antidepressant without psychotomimetic side effects. Transl Psychiatry 5:e632. https://doi.org/10.1038/tp.2015.136
62. Dong C, Zhang JC, Yao W, Ren Q, Ma M, Yang C, Chaki S, Hashimoto K (2017) Rapid and sustained antidepressant action of the mGlu2/3 receptor antagonist MGS0039 in the social defeat stress model: comparison with ketamine. Int J Neuropsychopharmacol 20(3):228–236. https://doi.org/10.1093/ijnp/pyw089
63. Sarkar A, Kabbaj M (2016) Sex differences in effects of ketamine on behavior, spine density, and synaptic proteins in socially isolated rats. Biol Psychiatry 80(6):448–456. https://doi.org/10.1016/j.biopsych.2015.12.025
64. Widman AJ, Stewart AE, Erb EM, Gardner E, McMahon LL (2018) Intravascular ketamine increases theta-burst but not high frequency tetanus induced LTP at CA3-CA1 synapses within three hours and devoid of an increase in spine density. Front Synaptic Neurosci 10:8. https://doi.org/10.3389/fnsyn.2018.00008
65. Pryazhnikov E, Mugantseva E, Casarotto P, Kolikova J, Fred SM, Toptunov D, Afzalov R, Hotulainen P et al (2018) Longitudinal two-photon imaging in somatosensory cortex of behaving mice reveals dendritic spine formation enhancement by subchronic administration of low-dose ketamine. Sci Rep 8(1):6464. https://doi.org/10.1038/s41598-018-24933-8
66. Sales AJ, Fogaca MV, Sartim AG, Pereira VS, Wegener G, Guimaraes FS, Joca SRL (2018) Cannabidiol induces rapid and sustained antidepressant-like effects through increased BDNF signaling and synaptogenesis in the prefrontal cortex. Mol Neurobiol 56:1070–1081. https://doi.org/10.1007/s12035-018-1143-4
67. Dunaevsky A, Tashiro A, Majewska A, Mason C, Yuste R (1999) Developmental regulation of spine motility in the mammalian central nervous system. Proc Natl Acad Sci U S A 96(23):13438–13443
68. Kwon HB, Sabatini BL (2011) Glutamate induces de novo growth of functional spines in developing cortex. Nature 474(7349):100–104. https://doi.org/10.1038/nature09986
69. MacLusky NJ, Luine VN, Hajszan T, Leranth C (2005) The 17alpha and 17beta isomers of estradiol both induce rapid spine synapse formation in the CA1 hippocampal subfield of ovariectomized female rats. Endocrinology 146(1):287–293. https://doi.org/10.1210/en.2004-0730
70. Dos Santos M, Salery M, Forget B, Garcia Perez MA, Betuing S, Boudier T, Vanhoutte P, Caboche J et al (2017) Rapid synaptogenesis in the nucleus accumbens is induced by a single cocaine administration and stabilized by mitogen-activated protein kinase interacting kinase-1 activity. Biol Psychiatry 82(11):806–818. https://doi.org/10.1016/j.biopsych.2017.03.014
71. Spruston N (2008) Pyramidal neurons: dendritic structure and synaptic integration. Nat Rev Neurosci 9(3):206–221. https://doi.org/10.1038/nrn2286
72. Yang C, Hu YM, Zhou ZQ, Zhang GF, Yang JJ (2013) Acute administration of ketamine in rats increases hippocampal BDNF and mTOR levels during forced swimming test. Ups J Med Sci 118(1):3–8. https://doi.org/10.3109/03009734.2012.724118
73. Song M, Martinowich K, Lee FS (2017) BDNF at the synapse: why location matters. Mol Psychiatry 22(10):1370–1375. https://doi.org/10.1038/mp.2017.144
74. Treccani G, Gaarn du Jardin K, Wegener G, Müller HK (2016) Differential expression of postsynaptic NMDA and AMPA receptor subunits in the hippocampus and prefrontal cortex of the flinders sensitive line rat model of depression. Synapse 70(11):471–474. https://doi.org/10.1002/syn.21918
75. Abildgaard A, Solskov L, Volke V, Harvey BH, Lund S, Wegener G (2011) A high-fat diet exacerbates depressive-like behavior in the Flinders Sensitive Line (FSL) rat, a genetic model of depression. Psychoneuroendocrinology 36(5):623–633. https://doi.org/10.1016/j.psyneuen.2010.09.004
76. Eriksson TM, Delagrange P, Spedding M, Popoli M, Mathe AA, Ogren SO, Svenningsson P (2012) Emotional memory impairments in a genetic rat model of depression: involvement of 5-HT/MEK/Arc signaling in restoration. Mol Psychiatry 17(2):173–184. https://doi.org/10.1038/mp.2010.131

77. Gomez-Galan M, De Bundel D, Van Eeckhaut A, Smolders I, Lindskog M (2013) Dysfunctional astrocytic regulation of glutamate transmission in a rat model of depression. Mol Psychiatry 18(5):582–594. https://doi.org/10.1038/mp.2012.10
78. Shiraishi Y, Mizutani A, Mikoshiba K, Furuichi T (2003) Coincidence in dendritic clustering and synaptic targeting of homer proteins and NMDA receptor complex proteins NR2B and PSD95 during development of cultured hippocampal neurons. Mol Cell Neurosci 22(2):188–201
79. Pontrello CG, Sun MY, Lin A, Fiacco TA, DeFea KA, Ethell IM (2012) Cofilin under control of beta-arrestin-2 in NMDA-dependent dendritic spine plasticity, long-term depression (LTD), and learning. Proc Natl Acad Sci U S A 109(7):E442–E451. https://doi.org/10.1073/pnas.1118803109
80. Duman RS, Aghajanian GK (2012) Synaptic dysfunction in depression: potential therapeutic targets. Science 338(6103):68–72. https://doi.org/10.1126/science.1222939